# Predicting Internal White Oak (*Quercus alba*) Log Defect Features Using Surface Defect Indicator Measurements

Ralph E. Thomas

## Abstract

As hardwood trees grow and develop, surface defects such as limb stubs and wounds are overgrown and encapsulated into the tree. Evidence of these defects can remain on the tree's surface for decades and in many instances for the life of the tree. The location and severity of internal defects dictate the quality and value of products that can be obtained from logs. Thus, log surface defect indicators such as log diameter at defect and surface indicator width, length, and rise provide a viable means of estimating the location and severity of internal defects. Evaluation of white oak (*Quercus alba*) log defects revealed that good correlations exist between external indicators and internal features for most severe defect types. Weaker correlations were observed with less severe defect types, such as bark distortions and adventitious knots.

Accurate information about the size, shape, and location of internal hardwood log defects is the key to dramatically improving the quality and value of lumber sawn. Several researchers have examined the internal/external defect relationship for various hardwood and softwood species during the past 50 years. Given the recent development of computerized scanning systems capable of detecting log surface defects (Thomas et al. 2006), there is more interest in finding reliable internal defect prediction models. The implementation of these models, combined with scanning and detection software, promises to provide internal defect information using simple laser surface scanning technology.

Schultz (1961) studied German Beech (*Fagus sylvatica*) and found that the ratio of the bark distortion width to distortion length was the same ratio of the stem when the branch stub was encapsulated to the current stem diameter. However, for species with heavier, irregular bark, Schultz found that it was difficult to judge the clear area above the defect using this method. Similarly, Shigo and Larson (1969) discovered that for many hardwoods the ratio of external defect height to width indicates the depth of the defect with respect to the radius of the stem at the defect.

Hyvärinen (1976) used sugar maple (*Acer saccharum*) data collected by Marden and Stayton (1970) to examine the correlation between external defect indicators and the internal features of grain orientation and defect encapsulation depth. The sugar maple data were collected from 44 trees obtained from three sites in upper Michigan. Hyvärinen found strong correlations among encapsulation depth and bark distortion width, length, and rise using linear regression methods. The best simple correlation ($r = 0.66$) was with diameter inside bark (DIB). The final model used stepwise multiple linear regression to find a strong correlation ($r = 0.74$) with DIB and distortion length to encapsulation depth.

Lemieux et al. (2001) conducted a similar study using 21 black spruce (*Picea mariana*) trees collected from a natural stand 75 km north of Quebec City. A total of 249 knot defects were dissected and the data recorded. It is interesting to note that the researchers found better correlations between external indicators and internal features on the middle and bottom logs than on the upper logs. Strong correlations ($r > 0.89$) were found among the length and width of internal defect zones and external features such as branch stub diameter. The researchers modeled the defects using three distinct zones corresponding to how the penetration angle changes over time in black spruce. The penetration angle is the angle at which a line through the center of the defect intersects the log surface. The Lemieux et al. study examined only branches that had not dropped or been pruned, thus preventing an examination of encapsulation depth.

The largest known study (Rast et al. 1973) examined correlations among external defect size and type populations and their impact on the grade of the lumber sawn from those logs. This study examined thousands of logs and several hardwood species. The results from this study were used to develop the hardwood tree and log grading rules. The correlation of external indicators to internal defects was limited to correlating log grade to lumber grade yield (Hanks 1976). Although very useful, this study only grossly considered the relationships among external and internal defects.

However, the traditional approach to locating internal log defects has been to experiment with X-ray/computed tomography (CT) or magnetic resonance imaging (MRI; Chang 1992, Sarigul et al. 2003). Typically, this research used medical CT scanners that were modified for industrial use. However, CT scanning technology remains expensive and has slower data acquisition rates than mill processing speed. Further, the technology has difficulty with larger diameter logs and log moisture content variations.

This research seeks to develop an alternative to CT scanning for locating and determining the size and shape of internal log defects using external indicators. In earlier studies internal prediction models for yellow-poplar (*Liriodendron tulipifera*; Thomas 2008), red oak (*Quercus rubra*; Thomas, in press a), and red oak and yellow-poplar knot clusters (Thomas 2009a) were developed. A recent validation sample used a sample of four red oak logs that were scanned and the defects manually identified and recorded (Thomas 2011). The logs were then sawn on a portable sawmill, and the position of all boards were tracked and recorded. Sawmill sawing solutions were replicated on the computer with the RAYSAW (Thomas, in press b) sawing simulator. The position and size of all knot defects on the actual boards were compared with their virtual counterparts. Overall, the models predicted the occurrence of 67 of 83 total defects, an accuracy rate of 80.7 percent. The median error of the measured distance between the actual defect location and the predicted defect location was 0.875 inch. The model's predictions for internal defect size were not as accurate. The median errors for predicting the width and length of a knot defect on a board surface were 1.25 and 0.37 inches, respectively.

Initially, it was believed that white and red oak log defect structures would be similar and that a combined model for both oak species could be developed. However, weaker correlations were observed for all defect types within the pooled species model. In addition, correlations for some features that were significant for either species separately were not significant within the pooled model. Thus, the creation of a separate white oak model became necessary.

## Methods

### Sample collection

White oak (*Quercus alba*) defect samples were collected from three sites in West Virginia: The Fernow Experimental Forest located near Parsons, West Virginia, and two forests managed by Mead-Westvaco located in Fayette County, West Virginia, named Fayette-1 and Fayette-2. Thirty-two trees were randomly selected from the Fernow site and 15 and 16 trees were randomly selected from the Fayette-1 and Fayette-2 sites, respectively. Each tree was bucked into log lengths, and the logs were laser-scanned and manually diagrammed, recording the location and type of all defects. The goal was to randomly collect four defects of each type from each tree whenever possible. For example, if there were eight sound knots on a tree, every second knot would be selected. Of course, not all trees have four defects of every type. In other cases, selecting one defect would prevent another from being selected due to defect overlap. In these cases, preference went to the least common defect type on that tree, and a different occurrence of the second defect type was used, if available. The number of defect samples of each defect type obtained from each site is shown in Table 1.

### Sample processing

All surface defects were identified according to the characteristics defined in *Defects in Hardwood Timber* (Carpenter et al. 1989). Once a surface defect was located and classified, the section containing the defect was cut from the log. Typically, the defect sections range from 12 to 24 inches in length. If, upon dissection, the inner portion of the defect was not completely contained within the section, the sample was discarded. For each sample the following information was recorded: defect type, surface width (across grain), surface length (along grain), ring count at defect location, log diameter at defect location, and bark thickness. Next, a groove was cut into the top of the sample along the line from the center of the defect to the pith of the sample. The groove is used to measure the rake angle of the defect as it penetrates into the log sample and can be seen in Figure 1. The sample was then flat sawn into 1-inch-thick slices. This resulted in a photo series showing the defect penetrating the log (Fig. 1). The entire collection of defect photo series for all species processed can be found in the Hardwood Log Defect Photographic Database (Thomas 2009b). For each slice, the depth (including any previous saw kerfs, slices, and bark slab), defect width, length, and distance of defect center to notch bottom was recorded. When a defect terminated between slices, it was assumed that it terminated at the halfway point through the slice.

### Modeling statistics

A series of $\chi^2$ tests were used to test for outliers in the internal/external data set (Komsta 2005). Any data points

Table 1.—*Types and numbers of all defects collected by site and overall.*

| Defect type | Location | | | Total |
|---|---|---|---|---|
| | Fernow | Fayette-1 | Fayette-2 | |
| Adventitious knot (AK) | 41 | 11 | 23 | 75 |
| Adventitious knot cluster (AKC) | 82 | 21 | 75 | 178 |
| Bump (BUMP) | 30 | 11 | 14 | 55 |
| Heavy distortion (HD) | 31 | 6 | 12 | 49 |
| Light distortion (LD) | 41 | 7 | 26 | 74 |
| Medium distortion (MD) | 31 | 7 | 11 | 49 |
| Overgrown knot (OK) | 98 | 39 | 59 | 196 |
| Overgrown knot cluster (OKC) | 33 | 17 | 28 | 78 |
| Sound knot (SK) | 33 | 7 | 5 | 45 |
| Sound knot cluster (SKC) | 19 | 9 | 9 | 37 |
| Unsound knot (UK) | 23 | 0 | 8 | 31 |
| Unsound knot cluster (UKC) | 1 | 1 | 2 | 4 |
| Total | 463 | 136 | 272 | 871 |
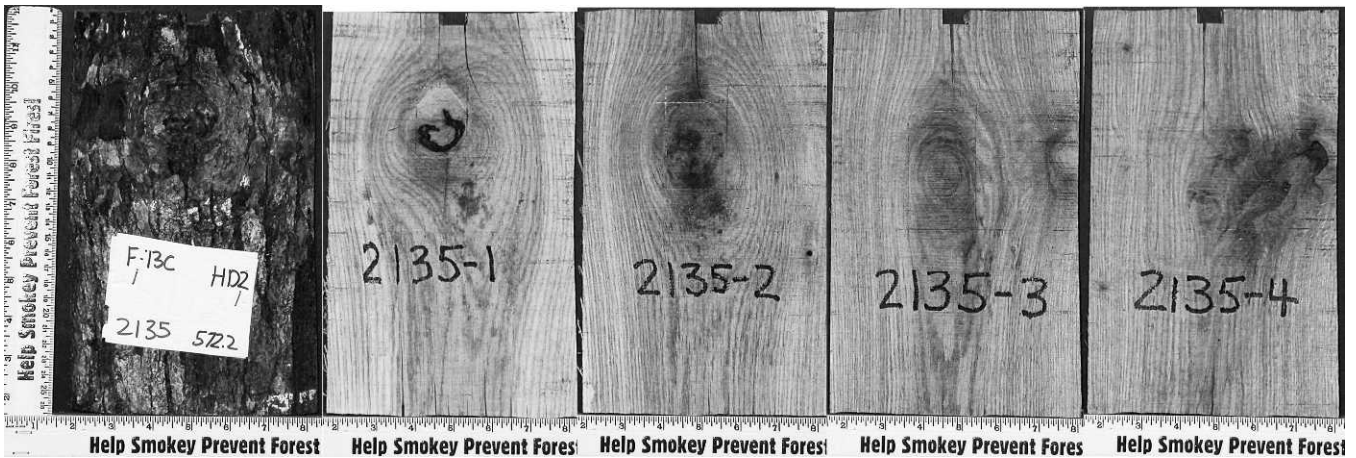
Figure 1.—Series of internal defect sections for a heavy bark distortion defect surface indicator.

identified as potential outliers were re-measured using the original sample for verification and corrected, if necessary. The data were grouped by defect type. With the R statistical analysis program (R Development Core Team 2006), stepwise multiple linear regression analyses were used to test for correlations among surface indicators and internal features. The independent variables used were surface indicator width (SWID), length (SLEN), rise (SRISE), and log diameter (DIB). These variables were selected because they are measurable during log surface inspection. Surface area (SWID × SLEN), volume (SWID × SLEN × SRISE), $SLEN^2$, $SRISE^2$, $SWID^2$, and all combinations of independent variables were examined as potential predictor variables. The dependent variables selected were penetration angle (RAKE), clear wood above defect (EDEPTH), total depth (TDEPTH), halfway point cross-section width (HWID), and halfway point cross-section length (HLEN). The halfway point is the geometric midpoint between the surface and total defect penetration depth. With these variables, an internal model of a defect can be constructed, and an approximate internal location can be determined (Fig. 2).
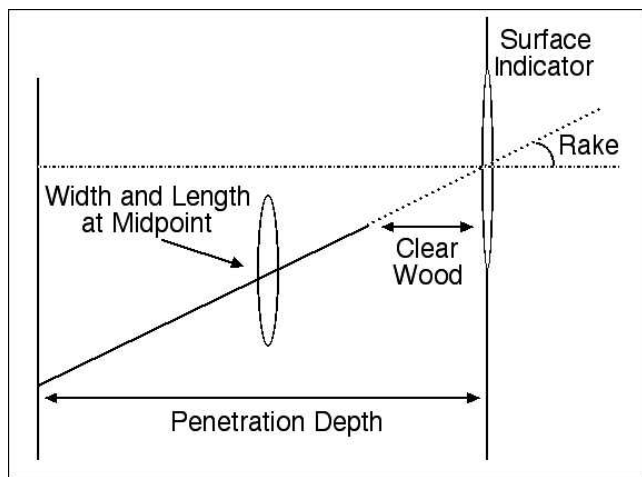
Within each defect type class, the data were randomly partitioned into two groups using the caTools package (Tuszynski 2006) for *R*. The first group contains approximately 66.7 percent of the sample and was used for model development and determining the internal/external feature correlation statistic (model development set). The second set contained the remaining records and was used for testing the prediction models (model validation set). Table 2 shows the numbers of observations used in the model development and testing steps. Note that similar defect types, bark distortions, for example, were grouped to increase sample sizes for model development and testing.

## Results and Discussion

Correlation results among external and internal features for all defects over the entire sample of each defect type or grouped type is presented in Table 3. The weakest correlations ($R^2 < 0.20$) were observed with the adventitious knots (AK) and adventitious knot cluster (AKC) defects. The internal features of the AK and AKC defects were highly variable, often appearing and disappearing at random. Because of the poor overall correlations among internal and external features, no predictive model was developed for the adventitious defects.

The heavy, medium, and light distortion defects (HD, MD, and LD, respectively) had stronger external/internal defect feature correlations than the adventitious defects



Figure 2.—Illustration of internal features predicted by the model.

Table 2.—Numbers of observations used in model development and testing by defect type.

| Defect type[a] | No. of observations | | |
| --- | --- | --- | --- |
| | Model data set | Testing data set | Total no. of observations |
| BUMP | 36 | 19 | 55 |
| Knot clusters | 79 | 40 | 119 |
| LD | 49 | 25 | 74 |
| All distortions | 113 | 59 | 172 |
| OK | 130 | 66 | 196 |
| OKC | 52 | 26 | 78 |
| All sound knots | 162 | 81 | 243 |

[a] LD = light distortion; OK = overgrown knot; OKC = overgrown knot cluster.

THOMAS

*Table 3.—Overall correlation results among external indicators and internal features for all samples.[a]*

| Defect type | Internal feature | $R^2$ | Correlation significant? | Residuals | | | |
|---|---|---|---|---|---|---|---|
| | | | | MAE | Min | Mean | Max |
| AKC | HWID | 0.13 | Y | 0.45 | −0.87 | −0.14 | 3.19 |
| | HLEN | 0.10 | Y | 0.51 | −1.68 | −0.14 | 3.32 |
| | RAKE | 0.07 | Y | 4.42 | −10.05 | −1.85 | 30.52 |
| | TDEPTH | 0.55 | Y | 0.78 | −4.79 | 0.20 | 2.28 |
| | EDEPTH | 0.13 | Y | 0.36 | −0.71 | −0.10 | 2.85 |
| AK | HWID | 0.04 | N | 0.29 | −0.57 | −0.11 | 1.40 |
| | HLEN | 0.15 | Y | 0.31 | −0.76 | −0.10 | 1.61 |
| | RAKE | 0.32 | Y | 4.24 | −16.27 | −0.84 | 29.71 |
| | TDEPTH | 0.28 | Y | 0.96 | −3.56 | 0.10 | 2.97 |
| | EDEPTH | 0.14 | Y | 0.76 | −1.50 | −0.25 | 4.70 |
| BUMP | HWID | 0.35 | Y | 0.46 | −1.22 | −0.09 | 1.67 |
| | HLEN | 0.29 | Y | 0.94 | −2.84 | −0.05 | 3.96 |
| | RAKE | 0.21 | Y | 13.27 | −33.47 | −2.56 | 34.61 |
| | TDEPTH | 0.79 | Y | 0.60 | −2.25 | 0.05 | 1.74 |
| | EDEPTH | 0.11 | N | 0.52 | −0.83 | −0.27 | 3.42 |
| HD | HWID | 0.40 | Y | 0.33 | −0.81 | −0.04 | 0.92 |
| | HLEN | 0.19 | Y | 0.56 | −1.00 | −0.14 | 2.50 |
| | RAKE | 0.04 | N | 8.14 | −14.40 | −2.33 | 23.42 |
| | TDEPTH | 0.76 | Y | 0.58 | −1.98 | 0.04 | 1.57 |
| | EDEPTH | 0.03 | N | 0.40 | −0.61 | −0.25 | 2.14 |
| MD | HWID | 0.38 | Y | 0.34 | −0.76 | 0.03 | 1.15 |
| | HLEN | 0.42 | Y | 0.55 | −1.14 | 0.02 | 1.43 |
| | RAKE | 0.23 | Y | 9.78 | −21.03 | −0.57 | 23.38 |
| | TDEPTH | 0.61 | Y | 0.75 | −2.61 | 0.26 | 1.72 |
| | EDEPTH | 0.12 | N | 0.54 | −1.02 | −0.10 | 1.77 |
| LD | HWID | 0.42 | Y | 0.33 | −1.09 | 0.09 | 0.72 |
| | HLEN | 0.26 | Y | 0.69 | −1.88 | −0.03 | 1.69 |
| | RAKE | 0.09 | N | 10.09 | −26.12 | −0.02 | 31.47 |
| | TDEPTH | 0.67 | Y | 0.67 | −2.70 | 0.04 | 1.57 |
| | EDEPTH | 0.19 | Y | 0.95 | −2.21 | 0.01 | 3.19 |
| OK | HWID | 0.53 | Y | 0.43 | −1.29 | −0.03 | 1.53 |
| | HLEN | 0.48 | Y | 0.95 | −2.48 | −0.09 | 4.33 |
| | RAKE | 0.35 | Y | 12.60 | −38.56 | 0.94 | 30.92 |
| | TDEPTH | 0.53 | Y | 0.76 | −4.54 | 0.10 | 4.02 |
| | EDEPTH | 0.01 | N | 0.01 | −0.02 | −0.01 | 0.98 |
| OKC | HWID | 0.60 | Y | 0.51 | −1.55 | 0.04 | 2.19 |
| | HLEN | 0.70 | Y | 0.84 | −2.35 | 0.05 | 2.48 |
| | RAKE | 0.39 | Y | 11.31 | −31.65 | −1.29 | 34.67 |
| | TDEPTH | 0.69 | Y | 0.54 | −1.74 | 0.09 | 2.21 |
| | EDEPTH | — | — | — | — | — | — |
| SK | HWID | 0.71 | Y | 0.25 | −0.68 | −0.01 | 0.98 |
| | HLEN | 0.66 | Y | 0.47 | −1.40 | 0.03 | 2.72 |
| | RAKE | 0.29 | Y | 8.25 | −14.96 | −2.39 | 40.63 |
| | TDEPTH | 0.61 | Y | 0.69 | −2.01 | 0.17 | 2.18 |
| | EDEPTH | — | — | — | — | — | — |
| SKC | HWID | 0.78 | Y | 0.29 | −0.70 | −0.03 | 0.85 |
| | HLEN | 0.66 | Y | 0.47 | −1.08 | −0.13 | 1.67 |
| | RAKE | 0.36 | Y | 6.56 | −20.51 | −1.65 | 22.33 |
| | TDEPTH | 0.41 | Y | 0.71 | −2.75 | 0.26 | 1.89 |
| | EDEPTH | — | — | — | — | — | — |
| UK | HWID | 0.74 | Y | 0.50 | −0.96 | −0.15 | 1.41 |
| | HLEN | 0.60 | Y | 0.97 | −2.56 | −0.02 | 2.85 |
| | RAKE | 0.74 | Y | 6.81 | −22.39 | 0.75 | 16.65 |
| | TDEPTH | 0.44 | Y | 0.74 | −2.17 | −0.21 | 2.07 |
| | EDEPTH | — | — | — | — | — | — |

[a] Defect type abbreviations are explained in Table 1. MAE = mean absolute error, Min = minimum; Max = maximum; Y = yes; N = no; HWID = halfway point cross-section width; HLEN = halfway point cross-section length; RAKE = penetration angle; TDEPTH = total depth; EDEPTH = clear wood above defect.

(Table 3). However, the number of samples for the HD and MD defects was not enough to support the development of strong defect type specific models (Table 3). Thus, the HD, MD, and LD data were pooled into a single all distortions group. The potential of grouping just the HD and MD defects together was explored, but correlations within the all distortions group were stronger than within the HD and MD grouped set. Correlation

results for LD defects are presented along with the results for the all distortions set.

Similarly, the clustered knot defects (overgrown [OKC], sound [SKC], and unsound [UKC]) were grouped together to obtain a sample large enough for model development and testing. In addition, a sound knot grouping was created for the overgrown knot (OK) and sawn knot (SK) defect samples because of the relatively low sample size of SK defects. Results for OK defects and the SK grouping are presented separately.

## Knot and knot cluster defects

Knots are sawn or broken-off limbs, dead or green, protruding, flush, or depressed, but with sound or rotten wood (Carpenter et al. 1989). A knot cluster is the occurrence of two or more knots together. Knots and knot clusters are considered degrade defects in all log grades. In veneer logs, knots are admitted if they are no more than 10 inches from either or both ends (Carpenter et al. 1989).

Model development with the severe knot defects discovered significant correlations ($\alpha < 0.01$) in all cases (Table 4). Overall, model development correlations with the pooled cluster knot data were slightly lower than those of the OKC defects. However, the mean absolute error (MAE) with the pooled data was slightly lower in most cases than with the OKC defect group. The one exception was with TDEPTH; here the correlation with surface features was the same for the OKC and pooled knot cluster data ($R^2 = 0.71$) with a MAE difference of only 0.04 inch (Table 4).

A comparison of the model development results for the OK and all sound knots grouping shows that correlations (multiple adjusted $R^2$) and error factors are approximately the same. This is reasonable because of the large proportion (80%) of OK defect samples in the all sound knots group. In addition, the correlations for all four internal variables, among external indicators and internal feature measurements, were stronger with the all sound knot group (Table 4).

Testing of the developed models for all of the knot defects and groupings (OK, OKC, all sound knots, and knot clusters) showed that the correlations remained significant for all variables. In addition, the differences between the model development and model testing MAEs were slight, with a maximum difference of 0.28 inch for TDEPTH and 5.21° for RAKE (Table 4).

The single defect types, OK and OKC, had fewer significant independent variables for each internal feature than did the grouped data sets: knot clusters and all sound knots (Table 5). DIB and SLEN were the most common significant variables for OK internal features ($\alpha < 0.01$), while SWID and SLEN were most common for OKC internal defect features. Not only did the grouped data sets have more significant independent variables, but interaction variables were more common as well. Eight of nine internal features for the grouped knot data sets had one or more significant interaction variables (Table 5).

## Bark distortions

Bark distortions are defects without any surface rise on a log face and are characterized by only swirled patterns in the bark that break or distort the normally straight grained bark pattern. Heavy distortions (HD) have the greatest degree of swirled bark, light distortions (LD) the least. As the tree grows the swirled pattern is stretched and broken and an HD progresses to a medium distortion (MD) and eventually to an LD.

Overall, most correlations for the individual distortion defects using the entire data sets among external indicator and internal feature measurements were significant ($\alpha < 0.01$). However, only with the LD defect set was a sample large enough to support model development and testing (Tables 1 and 2). Only 49 samples each of HD and MD defects were collected from the 63-tree sample. To facilitate model development and testing for MD and HD defects, the data were pooled. Poor model development and testing results for the grouped MD and HD data led to the creation of the all distortions grouped data set.

All model development correlations (multiple adjusted $R^2$) among external indicators and internal features for the LD and all distortions sets were significant ($\alpha < 0.01$). Overall, model development correlation and error results were approximately the same between the LD-only model and the all distortions model. Greater multiple adjusted $R^2$ values were found with the HLEN, RAKE, and EDEPTH features with the LD data set. Correlation results for the HWID and TDEPTH features were equal between the LD and all distortions data sets.

For RAKE, TDEPTH, and EDEPTH, the LD and all distortions data sets had the same set of significant independent variables (Table 5). For the LD data set, SWID was the only significant independent variable for the HWID and HLEN features. SWID also was a significant variable for the all distortions data set for the HWID and HLEN features, along with other surface feature variables (Table 5).

Only the correlations with the TDEPTH internal feature were significant ($\alpha < 0.01$) under model testing with the LD data set. In this case, the correlation coefficient ($R$) among external indicators and TDEPTH was 0.82 with a MAE of 0.70 inch. Correlation results with the all distortions data set were better, with correlations for HWID, HLEN, and TDEPTH being significant ($\alpha < 0.01$). As with the LD-only data set, correlations for model testing with the RAKE and EDEPTH variables were not significant ($\alpha < 0.01$).

## Bumps

A bump is an abrupt protrusion on the log surface. These are sometimes categorized by size as low, medium, or high. A low bump is a swelling on the log surface with a height-to-length ratio from 1:12 to as much as 1:6. Medium bumps have height-to-length ratios from 1:6 to as much as 1:3, high bumps have slopes steeper than 1:3 (Carpenter et al. 1989). For the purposes of this study, all bumps were grouped together regardless of size or slope. Overall, the correlations (multiple adjusted $R^2$) among external indicators and internal features for bump defects were not as strong as those found with the knot and knot cluster defects. However, the strongest correlation with TDEPTH of all defects occurred with the bump defects ($R^2 = 0.79$; Table 3). All correlations with internal features using the entire bump data set were significant ($\alpha < 0.01$), with the exception of EDEPTH.

Bump defect model development correlation results for internal features were all significant ($\alpha < 0.01$). As with the overall correlation results, the strongest correlation with TDEPTH of all defects occurred with the bump defects ($R^2 = 0.81$; Table 4). Correlations with other internal features

THOMAS

*Table 4.—Model development and testing correlation results.[a]*

| Defect type | Dependent variable | Model development results | | | Model testing results | | |
|---|---|---|---|---|---|---|---|
| | | Multiple adjusted $R^2$ | Mean absolute error | Correlation significant? | Correlation coefficient $R$ | Mean absolute error | Correlation significant? |
| Bump | HWID | 0.31 | 0.43 | Y | 0.36 | 0.61 | N |
| | HLEN | 0.31 | 0.98 | Y | 0.33 | 1.56 | N |
| | RAKE | 0.32 | 12.74 | Y | 0.04 | 16.39 | N |
| | TDEPTH | 0.81 | 0.57 | Y | 0.87 | 0.67 | Y |
| | EDEPTH | 0.10 | 0.36 | Y | 0.11 | 0.74 | N |
| Clusters | | | | | | | |
| (OKC + SKC + UKC) | HWID | 0.59 | 0.47 | Y | 0.79 | 0.53 | Y |
| | HLEN | 0.65 | 0.83 | Y | 0.87 | 0.83 | Y |
| | RAKE | 0.27 | 11.33 | Y | 0.70 | 11.62 | Y |
| | TDEPTH | 0.71 | 0.53 | Y | 0.75 | 0.73 | Y |
| | EDEPTH | — | — | — | — | — | — |
| OKC | HWID | 0.63 | 0.51 | Y | 0.75 | 0.50 | Y |
| | HLEN | 0.70 | 0.92 | Y | 0.78 | 0.82 | Y |
| | RAKE | 0.45 | 11.78 | Y | 0.41 | 12.40 | N |
| | TDEPTH | 0.71 | 0.57 | Y | 0.80 | 0.74 | Y |
| | EDEPTH | — | — | — | — | — | — |
| All sound knots | | | | | | | |
| (OK + SK) | HWID | 0.58 | 0.44 | Y | 0.71 | 0.50 | Y |
| | HLEN | 0.51 | 0.96 | Y | 0.70 | 1.07 | Y |
| | RAKE | 0.43 | 12.16 | Y | 0.45 | 15.36 | Y |
| | TDEPTH | 0.54 | 0.79 | Y | 0.68 | 0.95 | Y |
| | EDEPTH | — | — | — | — | — | — |
| LD | HWID | 0.31 | 0.33 | Y | 0.39 | 0.44 | N |
| | HLEN | 0.32 | 0.61 | Y | 0.19 | 0.89 | N |
| | RAKE | 0.17 | 10.43 | Y | 0.21 | 10.98 | N |
| | TDEPTH | 0.67 | 0.67 | Y | 0.82 | 0.70 | Y |
| | EDEPTH | 0.18 | 0.95 | Y | 0.29 | 0.87 | N |
| All distortions | | | | | | | |
| (HD + LD + MD) | HWID | 0.31 | 0.33 | Y | 0.43 | 1.45 | Y |
| | HLEN | 0.30 | 0.64 | Y | 0.44 | 0.74 | Y |
| | RAKE | 0.09 | 9.98 | Y | 0.12 | 11.53 | N |
| | TDEPTH | 0.67 | 0.68 | Y | 0.78 | 0.71 | Y |
| | EDEPTH | 0.07 | 0.86 | Y | 0.15 | 0.87 | N |
| OK | HWID | 0.57 | 0.41 | Y | 0.60 | 0.49 | Y |
| | HLEN | 0.41 | 0.96 | Y | 0.68 | 1.02 | Y |
| | RAKE | 0.27 | 14.83 | Y | 0.48 | 12.66 | Y |
| | TDEPTH | 0.44 | 0.83 | Y | 0.71 | 0.83 | Y |
| | EDEPTH | — | — | — | — | — | — |

[a] Abbreviations are explained in Table 1 and the footnote to Table 3.

such as HLEN and HWID were not as strong as those discovered with other defect types. However, the correlations were stronger than those encountered with the LD-only and all distortions data sets. Model testing correlation results with the exception of TDEPTH failed to be significant ($\alpha <$ 0.01). However, the correlation coefficient with TDEPTH was the strongest model testing result of all defect types ($R$ = 0.87). The significant independent variables for TDEPTH are DIB and SWID $\times$ SLEN ($\alpha <$ 0.01; Table 5).

## Adventitious knots and knot clusters

Adventitious knots (AK) and adventitious knot clusters (AKC), sometimes referred to as adventitious bud clusters and epicormic branches, are buds found at points along the stem. They arise from latent buds of a young stem and persist for an indefinite number of years (Carpenter et al. 1989). These buds can become activated at any time in a tree's life in response to various stimuli. In construction and local-use logs, AK and AKC are not degrade defects. In factory and veneer grade logs, AK and AKC defects are considered degrade defects.

Overall, correlation results for AK and AKC defects using the entire data set were the weakest relationships discovered of all defect types examined (Table 3). Despite a sufficient sample size, 75 AK defects and 178 AKC defects (Table 1), model development and testing correlations were weak and failed to be significant for most variables ($\alpha <$ 0.01). Thus, these results are omitted from this study. AK and AKC defects often occur sporadically, appearing and disappearing as the defect is traced into the log. Because of this sporadic nature, it is difficult to predict internal features for these defects using external indicators.

## Summary

All model development correlations (multiple adjusted $R^2$) among external measurements and internal features were significant ($\alpha <$ 0.01; Table 4). More importantly, most correlations ($R$) with the model testing data sets were

Table 5.—*Significant independent variables used in model development and testing by defect type and internal feature.*[a]

| Defect type | Dependent variable | Significant independent variables |
|---|---|---|
| Bump | HWID | SLEN |
| | HLEN | DIB + SLEN + SLEN × SWID |
| | RAKE | DIB + SWID + SRISE + SWID × SRISE |
| | TDEPTH | DIB + SWID × SLEN |
| | EDEPTH | SRISE |
| **Clusters** | | |
| (OKC + SKC + UKC) | HWID | SWID + SWID × SRISE + SWID × DIB + SRISE × SLEN + DIB × SLEN |
| | HLEN | DIB + SWID + DIB × SWID + DIB × SLEN |
| | RAKE | DIB + SWID + SRISE |
| | TDEPTH | DIB + SLEN + SRISE + SLEN × SWID + SLEN × SRISE |
| | EDEPTH | — |
| OKC | HWID | SWID + SLEN + SRISE |
| | HLEN | SLEN + SRISE + SRISE × DIB |
| | RAKE | DIB + SRISE + DIB × SWID |
| | TDEPTH | DIB + SLEN × SRISE + DIB × SRISE |
| | EDEPTH | — |
| **All sound knots** | | |
| (OK + SK) | HWID | SWID + SRISE + DIB × SRISE |
| | HLEN | SWID + SLEN + SRISE + SWID × SLEN + SLEN × SRISE |
| | RAKE | DIB + SWID + SRISE + SWID × SLEN + SLEN × SRISE |
| | TDEPTH | DIB + SLEN |
| | EDEPTH | SWID + SRISE + SWID × SRISE |
| LD | HWID | SWID |
| | HLEN | SWID |
| | RAKE | DIB + SWID |
| | TDEPTH | DIB |
| | EDEPTH | DIB + SWID + SLEN + SWID × SLEN |
| **All distortions** | | |
| (HD + LD + MD) | HWID | SWID + SRISE + SWID × SRISE |
| | HLEN | SWID + SLEN + DIB |
| | RAKE | SWID + DIB |
| | TDEPTH | DIB |
| | EDEPTH | SWID + SLEN + DIB + SWID × SLEN |
| OK | HWID | DIB + DIB × SWID |
| | HLEN | DIB + DIB × SLEN |
| | RAKE | SRISE + SRISE × DIB |
| | TDEPTH | SWID × SLEN + SLEN × SRISE + DIB × SLEN |
| | EDEPTH | — |

[a] Defect type and dependent variable abbreviations are explained in Table 1 and the footnote to Table 3. SLEN = surface indicator length; DIB = diameter inside bark; SWID = surface indicator width; SRISE = surface indicator rise.

significant ($\alpha < 0.01$). The strongest correlations ($R^2 > 0.60$) were with the most severe defect types—clusters and OKC defects. Correlations with the all sound knots group and OK defects also were strong with small MAEs. The weakest correlations ($R^2 < 0.35$) were with the distortion and bump defects, with the exception of the TDEPTH feature of bump defects, which had the strongest model development and testing correlations (Table 4). Correlations with the AK and AKC defects were weak and did not support model development and testing (Table 5).

The most severe defects are generally the most recent ones on the tree. Thus, defect surface indicators for the severe defects provide the most clues about the nature of the defects encapsulated within the log. Distortions and bumps are defects that have existed long enough to become mostly encapsulated within the log. Surface indicators for these types of defects have been distorted and sloughed off to some extent by the growing tree. Thus, correlations are weaker among external indicators and internal features for the less severe defects. This relationship also has been observed in yellow-poplar (Thomas 2008) and red oak (Thomas, in press a).

The goal of this research was to develop models capable of predicting internal defect features based on external defect characteristics. The results from this study indicate that most internal defects can be estimated using external feature data. To date, yellow-poplar, red oak, and white oak have been studied, resulting in the development of internal prediction models. These models will be further developed and tested using samples from additional sites. Models for additional hardwood species are in progress. A hardwood sawing program has been developed at West Virginia University that uses these defect models to predict lumber grade based on external log indicators and optimizes for maximum National Hardwood Lumber Association lumber grade value (Lin et al. 2011).

## Acknowledgments

## Literature Cited

Carpenter, R. D., D. L. Sonderman, and E. D. Rast. 1989. Defects in hardwood timber. Agriculture Handbook 678. US Department of Agriculture, Washington, D.C. 88 pp.

Chang, S. J. 1992. External and internal defect detection to optimize the cutting of hardwood logs and lumber. Transferring technologies to the hardwood industry. Handbook 3. US Department of Commerce, Beltsville, Maryland. ISSN 1064–3451.

Hanks, L. F. 1976. Hardwood tree grades for factory lumber. Research Paper NE-333. USDA Forest Service, Northeastern Forest Experiment Station, Newton Square, Pennsylvania. 31 pp.

Hyvärinen, M. J. 1976. Measuring quality in standing trees—Depth of knot-free wood and grain orientation under sugar maple bark distortions with underlying knots. PhD dissertation. University of Michigan, Ann Arbor. 142 pp.

Komsta, L. 2005. Outliers: Tests for outliers. R package version 0.12. http://www.komsta.net. Accessed February 10, 2012.

Lemieux, H., M. Beaudoin, and S. Y. Zhang. 2001. Characterization and modeling of knots in black spruce (*Picea mariana*) logs. *Wood Fiber Sci.* 33(3):465–475.

Lin, W., J. Wang, and R. E. Thomas. 2011. A 3D optimal sawing system for small sawmills in central Appalachia. *In:* General Technical Report P-78, Proceedings of the 17th Central Hardwood Forest Conference, S. Fei, J. M. Lhotka, J. W. Stringer, K. W. Gottschalk, and G. W. Miller (Eds.), April 5–7, 2010, Lexington, Kentucky; USDA Forest Service, Northern Research Station, Newtown Square, Pennsylvania. pp. 67–76.

Marden, R. M. and C. L. Stayton. 1970. Defect indicators in sugar maple: A photographic guide. Research Paper NC-37. USDA Forest Service, North Central Experiment Station, St. Paul, Minnesota. 29 pp.

Rast, E. D., D. L. Sonderman, and G. L. Gammon. 1973. A guide to hardwood log grading. General Technical Report NE-1. USDA Forest Service, Northeastern Forest Experiment Station, Upper Darby, Pennsylvania. 31 pp.

R Development Core Team. 2006. R: A language and environment for statistical computing. R Foundation for Statistical Computing, Vienna, Austria. ISBN 3-90051-07-0. http://www.R-project.org. Accessed February 10, 2012.

Sarigul, E., A. Abbott, and D. L. Schmoldt. 2003. Rule driven defect detection in CT images of hardwood logs. *In:* International Conference on Image Processing and Scanning of Wood, August 21, 2000, Mountain Lake, Virginia. pp. 37–49.

Schultz, H. 1961. Die Beurtilung der Qualitätsent-wickulung junger Bäume [The assessment of the quality development of young trees]. *Forstarchiv* 32:89–99.

Shigo, A. L. and E. vH. Larson. 1969. A photo guide to the patterns of discoloration and decay in living northern hardwood trees. Research Paper NE-127. USDA Forest Service, Northeastern Forest Experiment Station, Upper Darby, Pennsylvania. 100 pp.

Thomas, L., L. Milli, R. E. Thomas, and C. A. Shaffer. 2006. Defect detection on hardwood logs using laser scanning. *Wood Fiber Sci.* 38(4):682–695.

Thomas, R. E. 2008. Predicting internal yellow-poplar log defect features using surface indicators. *Wood Fiber Sci.* 40(1):14–22.

Thomas, R. E. 2009a. Modeling the relationships among internal defect features and external Appalachian hardwood log defect indicators. *Silva Fennica* 43(3):447–456.

Thomas, R. E. 2009b. Hardwood log defect photographic database software and user's guide. General Technical Report NRS-40. USDA Forest Service, Northern Research Station, Newtown Square, Pennsylvania. 21 pp.

Thomas, R. E. 2011. Validation of an internal hardwood log defect prediction model. *In:* General Technical Report P-78, Proceedings of the 17th Central Hardwood Forest Conference, S. Fei, J. M. Lhotka, J. W. Stringer, K. W. Gottschalk, and G. W. Miller (Eds.), April 5–7, 2010, Lexington, Kentucky; USDA Forest Service, Northern Research Station, Newtown Square, Pennsylvania. pp. 77–82.

Thomas, R. E. Predicting internal red oak (*Quercus rubra*) log defect features using surface indicator measurements. *In:* Proceedings of the 18th Central Hardwood Forest Conference (in press a).

Thomas, R. E. RAYSAW: A log sawing simulator for 3D laser-scanned hardwood logs. *In:* Proceedings of the 18th Central Hardwood Forest Conference (in press b).

Tuszynski, J. 2006. caTools: Miscellaneous tools; I/O, moving window statistics, etc. R package version 1.6. http://ncicb.nci.nih.gov/download/index.jsp. Accessed February 10, 2012.